RSC Advances

ROYAL SOCIETY OF CHEMISTRY

www.rsc.org/advances

RSC Advances

COMMUNICATION

Effects of Li Doping on the Negative Bias Stress Stability of Solution-processed ZnO Thin Film Transistors

Received 00th January 20xx,
Accepted 00th January 20xx

DOI: 10.1039/x0xx00000x

www.rsc.org/

Bokyung Kim,[a†], Si Yun Park,[a†] Jieun Ko,[a] Young-Jae Kim,[a*] and Youn Sang Kim[a,b*]

To investigate the effect of Li dopant on the electrical characteristics under negative bias stress (NBS), we analysed ZnO and Li doped ZnO TFTs under NBS with -20V for 10,800 s. The Li dopant enhanced the field effect mobility (8.21 $cm^2/V{\cdot}s$) and successfully sustained the variation of V_{on} of ZnO TFTs without any degradation of the field effect mobility.

The metal oxide semiconductors have been attracted as one of the most promising materials for the next generation displays including high resolution, transparent and flexible displays. The major benefits of metal oxides are the high electron mobility compared to amorphous silicon, the transparency in the visible spectrum, and the processibility of low-cost deposition methods at low-temperature compatible with polymer substrates.[1] Although indium-gallium-zinc oxide (IGZO), one of the most studied compositions in metal oxide semiconductors, was applied to switching components of ultra-high definition displays, indium has the substantial drawback of scarcity.

The general technique to deposit the metal oxide as the semiconductor layer in a thin film transistor (TFT) is vacuum deposition such as radio frequency (RF) sputtering[2], chemical vapour deposition (CVD)[3], and pulsed laser deposition (PLD)[4]. The metal oxide layer deposited by these vacuum processes has shown an excellent electrical performance. Despite the favourable electrical performance of the metal oxide layer from the vacuum techniques, the requirement of the high facility investment and non-continuous process are the primary handicap of the vacuum techniques in the next generation display. Thus, the solution-processed metal oxide semiconductors have been developed for the cost effective fabrication of large display panel without vacuum deposition,[5–7] but the high thermal energy is indispensable for oxidation and removing impurity in the solution process.[8,9] We previously reported the low-temperature and solution-processed zinc oxide (ZnO) films as a metal oxide semiconductor which were fabricated from carbon-free and indium-free materials. These ZnO films made from zinc ammine complex exhibited good electrical performance without any carbon-based organic residuals which act as obstacles of electron transport.[10] Add to these ZnO films, the novel alkali metal dopants for enhancement of the field effect mobility was reported. Especially, lithium (interstitial Li, Li_i) dopant (optimum doping concentration with 10 mol%) not only increased the field effect mobility of TFT over four times higher than that of ZnO TFTs, but also improved the stability of threshold voltage (V_{th}) under the positive bias stress.[11]

For practical liquid crystal display (LCD) applications, the stability of electrical characteristics under negative bias stress (NBS) takes priority over the stability under positive bias stress (PBS). Each transistor in a pixel of LCD panels is biased continuous AC pulse on the gate electrode, but a period of the turn-off time (negative gate voltage) is longer by two to three orders of magnitude than a period of the turn-on time (positive gate voltage) during a single frame time. For instance, the turn-on time is about 21 μs and the turn-off time is about 16.7 ms with frame rate of 60 Hz.[12] This prolonged NBS condition is the main source of the shift of V_{th} which causes serious non-uniform brightness. In case of an organic light emitting diode (OLED) display, it was reported that only 0.1V variation in V_{th} of driving transistor induces a 16% of luminance difference.[13] On the other, in case of LCD, over 0.8 V variation in V_{th} of TFT gradually makes the difference of grey colour.[14]

Herein, to address the NBS stability issue, we investigate the effect of Li dopant on the electrical characteristics stability of solution-processed ZnO TFTs under NBS (V_{gs} = -20 V) for 10,800 s. We respectively analysed the crystalline properties, the initial electrical characteristics, and the electrical characteristics stability after NBS of pristine ZnO and Li doped ZnO TFTs. In our comparative study, we found that Li dopant with the optimum concentration (10 mol%) does not distort the crystal structure of ZnO matrix, successfully enhances the initial field effect mobility and sustains the variation in V_{on} of ZnO TFTs without any degradation of the electrical characteristics after NBS.

[a] *Program in Nano Science and Technology, Graduate School of Convergence Science and Technology, Seoul National University, Seoul 151-742, Republic of Korea, E-mail: younskim@snu.ac.kr (Y. S. Kim), yjkim86@snu.ac.kr (Y.- J. Kim).*
[b.] *Advanced Institutes of Convergence Technology, 864-1 Iui-dong, Yeongtong-gu, Suwon-si, Gyeonggi-do 443-270, Republic of Korea.*
† Equally contributed to this work.
Electronic Supplementary Information (ESI) available: The Box charts of ZnO TFTs with various concentration, TEM images, output curves, and hysteresis of various ZnO TFTs. See DOI: 10.1039/x0xx00000x

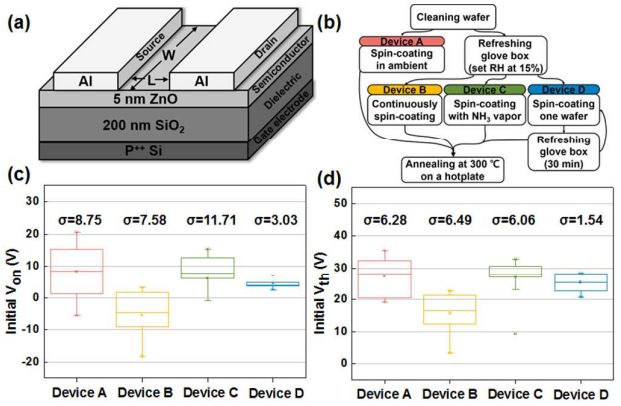

Figure 1. (a) The structure of ZnO/Li doped ZnO TFT (b) The semiconductor film preparation procedure. To investigate the influence of the spin-coating atmosphere conditions, the device A, B, C and D was coated in the four different conditions of the spin-coating atmosphere. (c) and (d) The box chart of initial V_{on} and V_{th} of ZnO TFTs made from various spin-coating atmosphere, respectively.

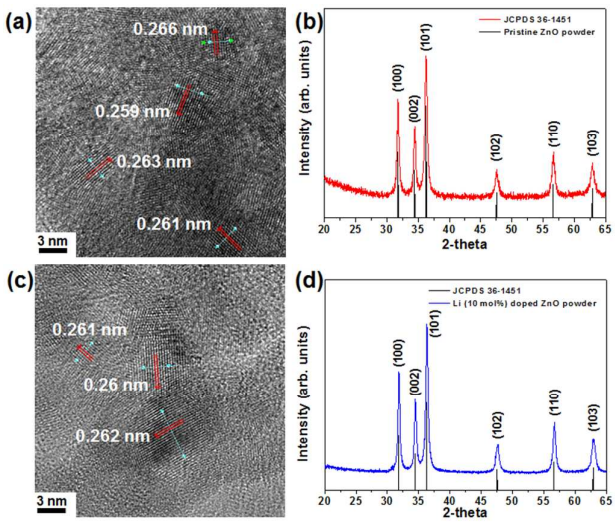

Figure 2. (a) and (c) The top view image of HR-TEM of pristine ZnO and Li (10 mol%) doped ZnO films, respectively. (b) and (d) The XRD patterns of pristine ZnO and Li (10 mol%) doped ZnO powder, respectively.

To obtain reliable TFTs (figure 1a) with small variations of initial V_{th}, we investigated optimized concentration of the zinc ammine complex solution and various conditions of the spin-coating atmosphere. According to our previous reports, the concentration of the zinc ammine complex solution was increased up to 90 mM.[15] We fabricated the ZnO film by spin-coating in a glove box using 83 mM and 90 mM of zinc ammine complex solution. The device from 83 mM and 90 mM zinc amine complex solution exhibited the standard deviation of 7.58 V and 13.76 V for initial V_{on} and 6.49 V and 9.27 V for initial V_{th}, respectively. The box charts of initial V_{on} and V_{th} of the device from 83 mM and 90 mM zinc ammine complex solution are shown in figure S1 (see the ESI). The second optimized parameter of ZnO TFT fabrication is the spin-coating conditions; the four different conditions of the spin-coating atmosphere (device A, B, C and D). The device A was spin-coated in the ambient condition and the other devices (device B, C and D) were spin-coated in the glove box with different ammonia vapour pressures. The device B was continuously spin-coated in the glove box without a refreshing air. Continuous spin-coating gradually fills the glove box with ammonia gas (NH_3) due to the high volatility of ammonia water. So, the coated ZnO film of device B could be affected by the high vapour pressure of ammonia gas and higher humidity compared to the coated ZnO film of device A. The device C was spin-coated in the glove box with a high vapour pressure of ammonia gas which was induced by placing the ammonia solution in the glove box. The device D was spin-coated in the glove box with a refreshing air (15% relative humidity) for 30 min after each coating. The flow chart of each process is shown in figure 1b and details for ZnO TFTs fabrication were described in the ESI. In this study, the turn-on voltage (V_{on}) was defined by the gate voltage (V_g) which induces 1 nA of drain current (I_d) with 60 V of drain voltage (V_d) and the threshold voltage (V_{th}) was extracted from the x-axis intercept of the linear fit to the ($\sqrt{I_d}$) versus V_g in the saturation region. Figure 1c and d showed the box charts of initial V_{th} and V_{on} of all devices. Device A, B, C, and D exhibited the standard deviation of 8.75 V, 7.58 V, 11.72 V, and 3.04 V for the initial V_{on} and 6.29 V, 6.49 V, 6.07 V, and 1.54 V for the initial V_{th}, respectively. These results confirmed that uncontrolled atmosphere of spin-coating process makes the large deviation of V_{th} and V_{on}. For NBS test, we fabricated and tested TFTs using 83 mM zinc ammine complex solution under the process condition of device D for stable operation-ability. Also, we used V_{on} instead of V_{th} because V_{th} values have inconsistency depending on defining the saturation region.

In order to investigate the effect of Li doping on the crystalline properties of ZnO thin film, high resolution transmission electron microscopy (HR-TEM) and X-ray diffraction (XRD) analyses were performed. Figure 2a and c showed the top view image of HR-TEM of pristine ZnO and Li (10 mol%) doped ZnO thin films. The nano-crystalline domains are clearly shown and the size of grains is less 10 nm. The lattice spacing of 0.262 nm and 0.261 nm was deduced from pristine ZnO and Li doped ZnO film, respectively. According to the lattice spacing of 0.260 nm for (002) ZnO crystal plane, we could speculate that our ZnO and Li doped ZnO films were oriented with the c-axis.[16] However, as shown in figure S2 (see the ESI), 20 mol% (over optimized doping concentration) of Li dopant clearly distorted crystalline structure of ZnO with c-axis orientation. As lattice spacing of 0.281 nm and 0.248 nm correspond to (100) and (101) ZnO crystal plane[16], 20 mol % of the Li doped ZnO film is randomly disordered with (100) and (101) planes of ZnO. The XRD analyses were performed with the ZnO and Li (10 mol%) doped ZnO powder because our ZnO film on the Si wafer could not be detected any substantial peak by grazing incidence XRD due to its thin thickness (about 5 nm). Figure 2b and d showed the XRD patterns of pristine ZnO powder and Li doped ZnO powder from the zinc ammine complex. The diffraction patterns exhibited three distinct peaks at 2 theta = 31.9°, 34.5°, and 36.6° indicating (100), (002), and (101) hexagonal ZnO crystal planes, respectively.[16] Since XRD patterns were obtained from ZnO powder, the intensity of (002) peak was weak compared to other crystal plane peaks. If XRD patterns had been obtained with ZnO thin films deposited on Si wafer, we could expect the strong (002) peak the same as previously report.[17] In accordance to the TEM results, we suggest that the Li dopant with optimum doping concentration (10 mol%) did not distort the crystallization of ZnO.

To investigate the effect of Li dopant on the stability of electrical characteristics (V_{on}, V_{th}, μ_{FE}, and S.S.) under NBS, a constant -20 V

(a)

Parameters	Average value of initial state				Average of delta value			
	V_{on} (V)	V_{th} (V)	μ_{FE} ($cm^2/V\cdot s$)	S.S. (V/decade)	ΔV_{on} (V)	ΔV_{th} (V)	$\Delta\mu_{FE}$ ($cm^2/V\cdot s$)	ΔS.S. (V/decade)
Pristine ZnO TFTs	4.25	26.21	4.35	1.98	-3.30	-2.48	+0.17	-0.72
Li dopd ZnO TFTs	-5.48	19.88	7.28	2.12	-3.84	-4.65	-0.31	-0.85

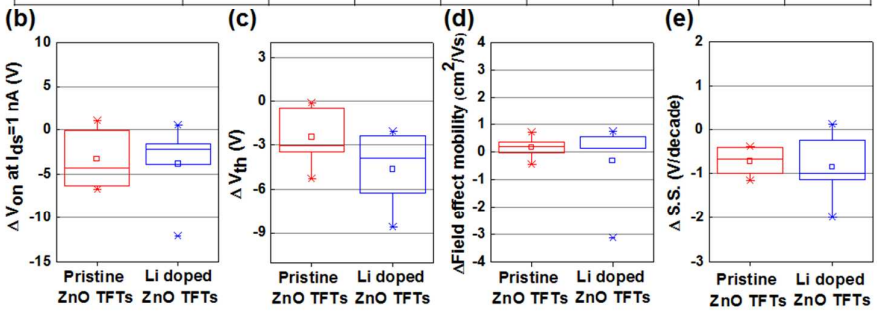

Figure 3. (a) The table showed the average of the initial state electrical characteristics and the average of the delta value of pristine ZnO TFTs and Li (10 mol%) doped ZnO TFTs after NBS (b~e) The box charts of pristine ZnO TFTs and Li (10 mol%) doped ZnO TFTs for the electrical characteristics induced by negative bias stress for 10,800 s (b) The variation of V_{on}, (c) The variation of V_{th}, (d) The variation of field effect mobility, and (e) The variation of subthreshold slope.

was biased on the gate electrode of pristine ZnO and Li (10 mol%) doped ZnO TFTs for 10,800 s. The measurement was performed under vacuum for eliminating the effect of instability by field-induced adsorption and desorption of oxygen molecules and water molecules.[18] Figure 3a showed the electrical characteristics of pristine ZnO and Li doped ZnO TFTs, which consist of the average of V_{on}, V_{th}, the field effect mobility (μ_{FE}) and the subthreshold slope (S.S.) of the initial state and the average of delta value after NBS. As expected, Li dopant increased the field effect mobility of Li doped ZnO TFTs compared to that of pristine ZnO TFTs. The maximum field effect mobility of Li doped ZnO TFT in the initial state was 8.21 $cm^2/V\cdot s$. In terms of the average subthreshold slope in the initial state, pristine ZnO and Li doped ZnO TFTs exhibited 1.98 and 2.12 V/decade, respectively. With these results, Li dopants increased the field effect mobility without any significant effects on the subthreshold slope in the initial state. After NBS, the subthreshold slope and the field effect mobility of both devices were improved. The average of the delta subthreshold slope of pristine ZnO and Li doped ZnO TFTs was -0.72 and -0.85 V/decade after NBS, respectively. Although the average of the delta field effect mobility of Li doped TFTs after NBS was -0.31 $cm^2/V\cdot s$ by one deteriorated device (Li doped ZnO TFT sample #1 in figure 4f), except the deteriorated sample #1 of Li doped ZnO TFT, all Li doped ZnO TFTs showed the increase of field effect mobility (figure 4f). We assume the uncontrolled humidity condition of annealing process could affect the one deteriorated device. As similar as the changes of the field effect mobility of Li doped ZnO TFTs, the average delta field effect mobility of pristine ZnO TFTs after NBS also slightly increased (0.17 $cm^2/V\cdot s$). The average of shifted V_{on} of pristine ZnO and Li doped ZnO TFTs was -3.3 V and -3.84 V and the average of shifted V_{th} was -2.48 V and -4.65 V, respectively. Although the difference of the average shifted V_{th} between pristine ZnO and Li doped ZnO TFTs was -2.17 V, but the difference of the average shifted V_{on} was only -0.54 V. In the other words, the pristine ZnO and Li doped ZnO TFTs have a similar tendency for the V_{on} shift under NBS. When the field effect mobility of Li doped ZnO TFTs is much higher than that of pristine ZnO TFTs, there wasn't any considerable difference in the V_{on} shift under NBS. Figure 3b~e showed the variation induced by NBS in V_{on}, V_{th}, the field effect mobility, and the subthreshold slope of both ZnO and Li doped ZnO TFTs in the form of the box chart, respectively. As shown in figure 3b~e, Li dopant with the optimum concentration (10 mol%) did not effect on the electrical characteristics of ZnO TFTs after NBS.

Figure 4a and d showed that the evolution of the transfer curves of pristine ZnO and Li doped ZnO TFTs, as a function of NBS time. The transfer curves showed a parallel shift of V_{on} in the negative direction without any significant changes of its shape. The output curves and hysteresis of the both devices after NBS were shown in figure S3 (see the ESI). The instability of metal oxide TFTs under bias stress could be elucidated by representative mechanisms: charge injection, charge trapping, state creation or ambient effect.[18–21] These mechanisms have different effect on the variation of V_{th}. The

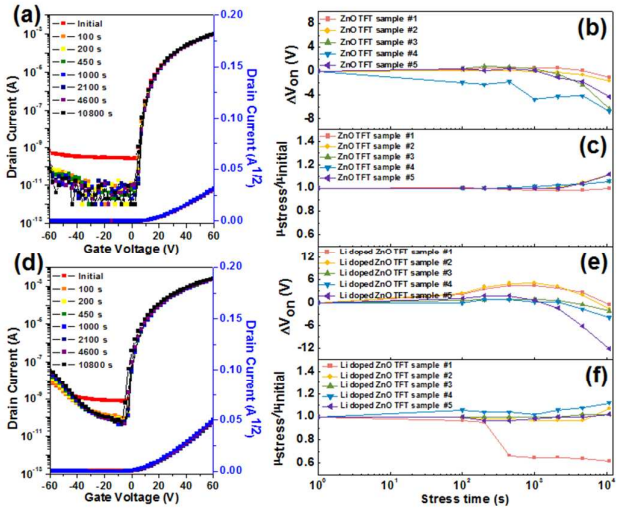

Figure 4. (a) and (d) The transfer curves of pristine ZnO TFT and Li (10 mol%) doped ZnO TFT, respectively under NBS condition, V_{ds} = GND and V_{gs} = -20 V for 10,800 s at room temperature. (b) and (c) The changes in V_{on} and the field effect mobility of pristine ZnO TFTs, respectively as function of negative bias stress time. (e) and (f) The changes in V_{on} and the field effect mobility of Li (10 mol%) doped ZnO TFTs, respectively as function of negative bias stress time.

charge injection model has a linear increase rate of ΔV_{th} versus logarithmic stress time and charge trapping has an exponential increase rate versus logarithmic stress time.[22] The state creation mechanism causes a large V_{th} shift by 10 V in case of the PLD deposited IGZO TFTs.[21] Also, the instability mechanism from the ambient effect on the non-passivation device is excluded owing to the measurement was performed in the vacuum chamber as mention above. Figure 4b and e showed the exponential increase of ΔV_{on} of ZnO and Li doped ZnO TFT versus logarithmic stress time and we speculated that the instability of our devices caused by charge trapping mechanism. The changes of the field effect mobility of both devices versus stress time were shown in figure 4c and f. The variations of the field effect mobility and the V_{on} of Li doped ZnO TFTs over stress time were similar to the results of ZnO TFTs. With these results, we assumed that Li dopant with optimized doping concentration with 10 mol% did not notably effect on the stability of electrical characteristics of ZnO TFTs under NBS, and it also had kept its higher field effect mobility. Therefore, the Li dopant could improve the field effect mobility without any changes of the variation in V_{on} of ZnO TFTs after NBS.

The slight shift of V_{on} of both devices in a negative direction is caused by trapping of accumulated positive charged ion (zinc interstitial (Zn_i) or oxygen vacancies from non-stoichiometric properties of ZnO) at the interface between semiconductor and dielectric layer.[23] The accumulation of positive charged ion is derived from the applied negative bias stress on the gate electrode of both devices. The Li dopant which plays a role of electron donor did not significantly affect the non-stoichiometric properties of ZnO because Li dopant with the optimum concentration prefers interstitial sites over substitution sites in the ZnO matrix. As the difference of the migration energy between Zn_i and Li_i is as small as 0.04 ~ 0.11 eV, we speculate that the effect of Zn_i and Li_i on the variation in V_{on} are quite similar.[24,25] Therefore, there could be no significant difference of V_{on} instability between pristine ZnO and Li doped ZnO TFTs.[10] Besides, the increase of the field effect mobility of both devices after NBS could be explained by additional carriers. The additional carriers are from positively charged donor state above the Fermi level due to band bending when the negative bias is applied.[23] The illustration of the band bending diagram is shown in figure S4 (see the ESI). Although other metal dopants such as Al, Y and Hf improved bias stress stability through suppressing the formation of oxygen vacancy, the field effect mobility was decreased due to reduction of carrier concentration.[26–28] However, Li dopant with optimized concentration drastically increased the field effect mobility of ZnO TFT and retained a little shift of V_{on} compared with that of pristine ZnO TFT after prolonged NBS. With these benefits of Li dopant which induces the high field effect mobility and negligible difference of V_{on} shift compared to pristine ZnO TFTs, Li could be a favourable dopant. If the bias stress stability of V_{on} of solution-processed metal oxide (such as ZnO) TFTs have been improved by passivation technology, [29] Li will be useful dopant for realizing low-cost fabricated high resolution LCD displays.

Conclusions

To investigate the effect of Li dopant on the electrical characteristics under NBS, we fabricated the solution processed pristine ZnO TFTs and Li (10 mol%) doped ZnO TFTs, then a constant -20 V was biased on the gate electrode of TFTs during 10,800 s. We deduced that Li dopant did not significantly influence on the electrical characteristics during NBS. The Li dopant enhanced the initial field effect mobility of pristine ZnO TFTs from 4.35 to 7.28 $cm^2/V{\cdot}s$ and did not aggravate the variation of the V_{on} of pristine ZnO TFTs under NBS without the degradation of other electrical characteristics. For practical HD LCD applications of metal oxide TFTs, the high field effect mobility and the low variation in V_{on} are a key factor, because the high field effect mobility alleviates a charging time issue for the capacitors in each scan line and the low variation of V_{on} prevents the non-uniform brightness problems induced by substantial variation of V_{on}. Combined with various techniques which improve the V_{on} stability of solution-processed metal oxide TFTs, the Li dopant could be an attractive dopant for a low-cost fabricated HD LCD because lithium effectively enhances the field effect mobility without degradation of V_{on} stability under NBS.

Acknowledgement

This work was supported by Basic Research Program (2011–0018113) of National Research Foundation (NRF) of Korea and Center for Advanced Soft Electronics as Global Frontier Research Program (2013M3A6A5073177) of the Ministry of Science, ICT and Future Planning of Korea.

Notes and references

1 K. Nomura, H. Ohta, A. Takagi, T. Kamiya, M. Hirano and H. Hosono, *Nature*, 2004, **432**, 488.
2 P. F. Carcia, R. S. McLean, M. H. Reilly and G. N. Jr, *Appl. Phys. Lett.*, 2003, **82**, 1117.
3 J. Zhu, H. Chen, G. Saraf, Z. Duan, Y. Lu and S. T. Hsu, *J. Electron. Mater.*, 2008, **37**, 1237.
4 S. Masuda, K. Kitamura, Y. Okumura, S. Miyatake, H. Tabata and T. Kawai, *J. Appl. Phys.*, 2003, **93**, 1624.
5 S. T. Meyers, J. T. Anderson, C. M. Hung, J. Thompson, J. F. Wager and D. A. Keszler, *J. Am. Chem. Soc.*, 2008, **130**, 17603.
6 K. Kim, S. Y. Park, K.-H. Lim, C. Shin, J.-M. Myoung and Y. S. Kim, *J. Mater. Chem.*, 2012, **22**, 23120.
7 Y. B. Yoo, J. H. Park, S. J. Lee, K. M. Song and H. K. Baik, *Jpn. J. Appl. Phys.*, 2012, **51**, 040201.
8 K. K. Banger, Y. Yamashita, K. Mori, R. L. Peterson, T. Leedham, J. Rickard and H. Sirringhaus, *Nat. Mater.*, 2011, **10**, 45.
9 M. Ohyama, H. Kouzuka and T. Yoko, *Thin Solid Films*, 1997, **306**, 78.
10 S. Y. Park, B. J. Kim, K. Kim, M. S. Kang, K.-H. Lim, T. I. Lee, J. M. Myoung, H. K. Baik, J. H. Cho and Y. S. Kim, *Adv. Mater.*, 2012, **24**, 834.
11 S. Y. Park, K. Kim, K.-H. Lim, E. Lee, S. Kim, H. Kim and Y. S. Kim, *RSC Adv.*, 2013, **3**, 21339.
12 J. K. Jeong, *J. Mater. Res.*, 2013, **28**, 2071.
13 Z. C. Feng, *Handbook of Zinc Oxide and Related Materials: Volume Two, Devices and Nano-Engineering*, CRC Press, 2012.
14 Y. Kuo and E. S. E. Division, *Thin Film Transistor Technologies V: Proceedings of the International Symposium*, The Electrochemical Society, 2001.

15 S. Y. Park, S. Kim, J. Yoo, K.-H. Lim, E. Lee, K. Kim, J. Kim and Y. S. Kim, *RSC Adv.*, 2014, **4**, 11295.
16 J. L. B. S. C. Abrahams, *Acta Crystallogr. B*, 1969, **25**, 1233.
17 B. S. Ong, C. Li, Y. Li, Y. Wu and R. Loutfy, *J. Am. Chem. Soc.*, 2007, **129**, 2750.
18 J. K. Jeong, H. Won Yang, J. H. Jeong, Y.-G. Mo and H. D. Kim, *Appl. Phys. Lett.*, 2008, **93**, 123508.
19 A. Suresh and J. F. Muth, *Appl. Phys. Lett.*, 2008, **92**, 033502.
20 R. B. M. Cross and M. M. De Souza, *Appl. Phys. Lett.*, 2006, **89**, 263513.
21 K. Nomura, T. Kamiya, M. Hirano and H. Hosono, *Appl. Phys. Lett.*, 2009, **95**, 013502.
22 J.-M. Lee, I.-T. Cho, J.-H. Lee and H.-I. Kwon, *Appl. Phys. Lett.*, 2008, **93**, 093504.
23 E. N. Cho, J. H. Kang, C. E. Kim, P. Moon and I. Yun, *IEEE Trans. Device Mater. Reliab.*, 2011, **11**, 112.
24 G.-Y. Huang, C.-Y. Wang and J.-T. Wang, *J. Phys. Condens. Matter*, 2009, **21**, 345802.
25 A. Janotti and C. G. Van de Walle, *Rep. Prog. Phys.*, 2009, **72**, 126501.
26 T. Jun, K. Song, Y. Jung, S. Jeong and J. Moon, *J. Mater. Chem.*, 2011, **21**, 13524.
27 W.-S. Kim, Y.-K. Moon, K.-T. Kim, S.-Y. Shin, B. Du Ahn, J.-H. Lee and J.-W. Park, *Electrochem. Solid-State Lett.*, 2010, **13**, H295.
28 C. H. Ahn, B. H. Kong, H. Kim and H. K. Cho, *J. Electrochem. Soc.*, 2011, **158**, H170.
29 S. An, M. Mativenga, Y. Kim and J. Jang, *Appl. Phys. Lett.*, 2014, **105**, 053507.